2021 43rd Annual International Conference of the
IEEE Engineering in Medicine & Biology Society (EMBC)
Oct 31 - Nov 4, 2021. Virtual Conference

Motion Artifact Resilient Cuff-Less Blood Pressure Monitoring Using a Fusion of Multi-Dimensional Seismocardiograms

Po-Ya Hsu,[1*] Po-Han Hsu,[1] Hsin-Li Liu,[2] Kuan-Yu Lin[2] & Tsung-Han Lee[1]

***Abstract*— Blood pressure (BP) monitoring is critical to raise awareness of hypertension and hypotension, yet the commonly used techniques require the person staying still along with a cuff around the arm. Some cuff-less approaches have been researched, but all hinder the person from moving around. To address the challenge, we propose using a fusion of accelerometers to achieve motion artifact resilient blood pressure monitoring. Such technique is accomplished with the motion artifact removal process and feature extraction from multi-dimensional seismocardiograms. The efficacy of our BP monitoring models is validated in 19 young healthy adults. Both the diastolic and systolic BP monitoring models fulfill the AAMI standard and British Hypertension Society protocol. For sitting still BP monitoring, the mean and standard deviation of diastolic and systolic difference errors (DE) are 0.09 ± 4.10 and -0.25 ± 5.45 mmHg; moreover, the mean absolute difference errors (MADE) are 3.62 and 4.73 mmHg. In walking motions, the DE are 1.15 ± 4.47 mmHg for diastolic BP and -0.38 ± 6.67 for systolic BP; furthermore, the MADE are 3.36 and 5.07 mmHg, respectively. The motion artifact resilient cuff-less BP monitoring reveals the potential of portable BP monitoring in healthcare environments.**

***Clinical relevance*— Monitoring blood pressures cuff-lessly during walking can significantly speed up the detection of cardiovascular disease and critically improve the healthcare environment.**

I. INTRODUCTION

Blood pressure (BP) is a pivotal indicator of the cardiovascular health status of a person. A large number of cardiovascular diseases is substantially related to abnormal BP values. Therefore, wearable BP monitors are in highly requirement to raise early awareness of hypertension and hypotension [1]. Nowadays, the frequently adopted techniques include auscultation [2], volume clamping [3], oscillometry [4], and applanation tonometry [5]. All the aforementioned methods require the usage of an inflatable cuff and the person staying still, which indicates the need of improvements in the current techniques.

Some cuff-less BP monitoring approaches have been proposed [6], [7], [8], [9]. According to Chang et al. [6] and Kim et al. [7], features extracted from seismocardiography (SCG) and ballistocardiography (BCG) can be employed to monitor BP. In Poon et al. 's [8] and Zheng et al.'s [9] studies, pulse transit time (PTT) is derived from electrocardiogram (ECG) and photoplethysmography (PPG) to compute BP. Although optimistic results are reported in these studies, the suggested strategies are prone to motion artifacts in the signals and some require further calibrations.

In this paper, we propose a motion artifact resilient BP monitoring model using a fusion of wearable accelerometers. We demonstrate the efficacy of the BP models in 20 young healthy adults. We contribute to:

- building a cuff-less BP monitoring model that fulfills the Association for the Advancement of Medical Instrumentation (AAMI) standard and British Hypertension Society protocol
- achieving motion artifact resilient BP monitoring
- devising robust SCG features for BP monitoring

II. METHODS

We first describe the data acquisition method and experimental design. Next, we elaborate on the sensor data processing step. Subsequently, we present the feature extraction approach and the construction of motion artifact resilient blood pressure monitoring model. Last, we specify how we quantify the performance of the proposed model compared to other existing methodology.

A. Data Acquisition

The current study was approved by the Jen-Ai Hospital-Joint Institutional Review Board. In this study, we recruited 20 young healthy volunteer to undergo the data acquisition process. All 20 subjects willingly provided the written informed consent to participate in the study. The age of the participants lies within $25-32$ years, and the gender distribution is 6 females and 14 males.

TABLE I
DESIGN OF EXPERIMENTS

Activities	sitting, standing, walking, sitting after walking
Duration	each activity lasts for 3 minutes
Sensor Placements	left/right wrists, heart, sternum, neck near left carotid artery
Description	participants wear the sensors throughout the whole experiment
Sensor	tri-axial accelerometers
Measurements	accelerations and blood pressure

We summarize the experimental design in Table I. All the participants went through the four activities: sitting still, standing still, walking at normal pace, and sitting right after walking. For each activity, the participant performs either

This work was not supported by any organization.

[1]Po-Ya Hsu, Po-Han Hsu and Tsung-Han Lee are with the Department of Computer Science & Engineering, University of California, San Diego, The USA

[2]Hsin-Li Liu and Kuan-Yu Lin are with the Department of Nursing, Central Taiwan University of Science and Technology, Taiwan

[*]Po-Ya Hsu is the corresponding author p8hsu@eng.ucsd.edu

the same posture or consistent motion (walking) for three minutes with the wearable sensors placed on the body.

The collected data include body acceleration, systolic blood pressure (SBP), and diastolic blood pressure (DBP). Throughout the whole experiment, the acceleration data are measured with the sensors placed on the participant's heart, sternum, left carotid, and bilateral wrists (as shown in Fig. 1). These body parts are chosen since it is very likely to measure the heart-induced signals at these locations. The acceleration sensors are MPU-6050, and the data sampling rate is set to 150Hz in our experiment. During the two sitting activities, the SBP and DBP data are collected using Rossmax MG150f. This blood pressure monitor was certified by European Society of Hypertension and clinically validated by British Hypertension Society with an A/A grade. All the data acquisition was completed by the same person, who was well trained by an experienced registered nurse to perform blood pressure measuring. Moreover, before the start of each activity, the person inspected all the sensors to be well-functioning and properly leveled. In the experiment, one subject's BP monitoring varies larger than 40 mmHg, and we remove this subject's data from BP model construction.

Fig. 1. Sensor placements in the study.

B. Signal Processing

We process the raw acceleration signals in four steps: 1) data normalization, 2) low-frequency noise removal, 3) high-frequency noise removal, and 4) data smoothing. To be more specific, the whole signal processing procedure is applied to each dimensional acceleration independently. In the first step, we compute the average of each dimensional acceleration and subtract the raw signal by this average so as to remove the gravity effect and other constant acceleration factor. This strategy was also adopted in [6]. In the second step, we make use of the third order Savitzky-Golay filter to clean the unwanted low-frequency signal. Such approach has been shown effective in removing motion artifact in [10]. In the third step, we remove the high-frequency noise with a sixth-order Butterworth lowpass filter. In the final step, we smooth the data through interpolating the processed signal with spline cubic curves at 750Hz. We portrait the raw and processed acceleration signals of the sensor located on top of the heart in Fig. 2.

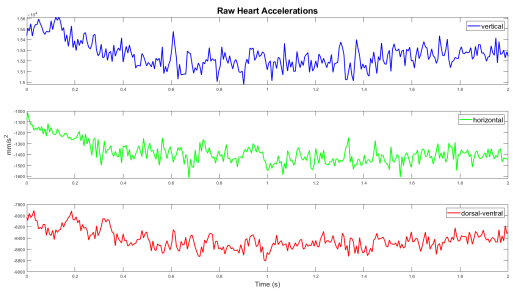

(a) Raw Data

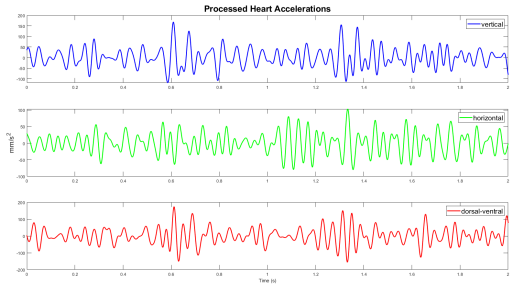

(b) Processed Data

Fig. 2. Demonstration of raw and processed data.

C. Feature Extraction

Our proposed feature extraction methodology is composed of two major pieces. One is heartbeat identification, and the other is feature construction. For the completion of the first piece, we leverage the methods used in [6] and [11] through a sophisticated combination of the two. In the primary step, we borrow the peak detection method applied in [6]. We select the valid heartbeats where the peaks are observed in both the vertical and dorsal-ventral accelerations with a tolerance of 10ms. Next, we derive the envelope of the dorsal-ventral acceleration and perform the waveform-based heartbeat detection as suggested in [11]. The envelope is constructed using spline interpolation over local maxima separated by at least 200ms, and each envelope packet is expected to enclose one heartbeat. Subsequently, we conduct a false positive removal and search-back for the missing heartbeats through the heartbeat period estimation method detailed in [11].

For feature extraction, we generate the representative waveform first and manipulate the fiducial point method to construct the feature space. As reported in several SCG related studies [6], [12], [13], due to the body motion artifacts, the SCG varies from heartbeat to heartbeat. Therefore, we strategically align five one-second consecutive acceleration waveform along the heartbeat peaks and treat the ensemble average of the five waveforms as the representative. We demonstrate the representative waveforms of each axial acceleration in Fig. 3.

After generating the representations, we search the peaks and valleys close to the heartbeat peak and specify them as the fiducial points. Next, we empirically select seven fiducial

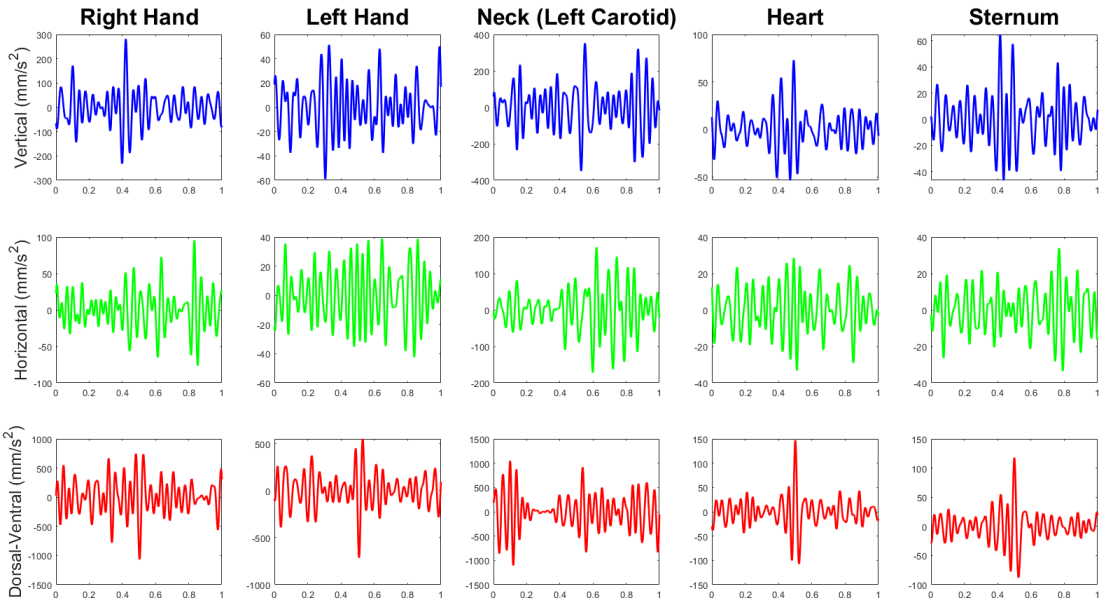

Fig. 3. Demonstration of the ensemble average acceleration waveforms.

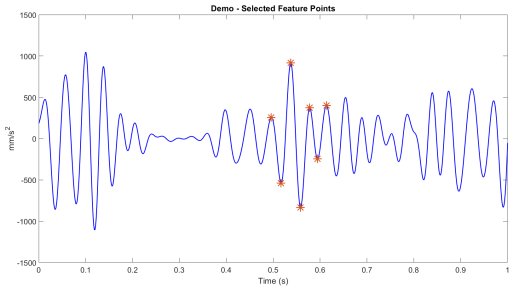

Fig. 4. Illustration of the selected fiducial points. The candidate features are the temporal duration and magnitude ratio between each two fiducial points.

points as illustrated in Fig. 4. Such selection strategy is based on the physiology of SCG/BCG curves, which usually contain the fiducial points H, I, J, K, L, M, N waves [7]. The heartbeat peak is chosen along with the preceding valley and peak and the two succeeding ones.

Last, we construct the feature space using the time interval and magnitude ratio between each pair of the fiducial points. Let's denote the time and the magnitude of the i^{th} and the j^{th} fiducial points as t_i, t_j and a_i, a_j. Then, we define our timing feature space as $t_j - t_i$ for all $j > i$, and we specify our magnitude feature space as $\frac{|a_i - a_j|}{M}$, where M is the largest magnitude of all pairs of fiducial points ($M := max(|a_i - a_j|) \forall i, j$). Given the fact that the acceleration magnitude varies drastically due to motions, we choose the magnitude ratio instead of the numerical value of the magnitude as our features.

D. Model Construction

We employ stepwise regression to build the proposed motion artifact resilient BP estimation model. Such model construction takes two steps to accomplish. Initially, we apply stepwise regression method to select the features that best estimate the BP for each dimensional acceleration. More specifically, only the accelerations from sitting activities are employed, and we construct two different models for systolic and diastolic blood pressures, respectively. Next, we utilize the ensemble of the chosen features from each acceleration together with the height and weight of the subjects as the predictors in the ultimate BP estimation model. Such BP estimation model is also established using stepwise regression and is regarded as the motion artifact resilient BP estimation model.

E. Performance Evaluation

We evaluate the model's performance by computing the difference errors (DE), mean absolute difference errors (MADE), and root-mean-square errors (RMSE). Furthermore, we conduct correlation analysis between the estimated and the measured BP.

For estimated BP in standing and walking activities, we compare the estimations with the averaged BP in the sitting activity through feeding the motion artifact resilient BP model with the standing and walking features.

III. Results & Discussion

We showcase the competitiveness of the proposed blood pressure estimation models in Table II, briefly discuss the DBP and SBP models subsequently, and last present the potential blood pressure monitoring system for human subjects during walking motion.

TABLE II

EVALUATION OF THE PROPOSED ACCELERATION-BASED BP MONITORING TECHNIQUE

	Diastolic Pressure	
Approach	M ± STD, RMSE, MADE	Correlation
Ours - sitting	0.09 ± 4.10 , 3.93, 3.62	$r = 0.80$
Ours - standing	0.93 ± 4.53 , 4.51, 3.30	$r = 0.72$
Ours - walking	1.15 ± 4.47 , 4.50, 3.36	$r = 0.59$
Tri-axial SCG [6]	-0.02 ± 3.82 , 3.82, –	$r = 0.97$
BCG-based [7]	–, 5.7, –	$r = 0.80$
PTT-based [8]	0.9 ± 5.6, – , –	–
	Systolic Pressure	
Ours - sitting	-0.25 ± 5.45 , 5.17, 4.73	$r = 0.81$
Ours - standing	-0.36 ± 6.26 , 6.11, 4.98	$r = 0.72$
Ours - walking	-0.38 ± 6.67 , 6.51, 5.07	$r = 0.70$
Tri-axial SCG [6]	-0.59 ± 7.46 , 5.57, –	$r = 0.96$
BCG-based [7]	–, 7.3, –	$r = 0.78$
PTT-based [8]	0.6 ± 9.8, – , –	–
PTT-based [9]	2.8 ± 8.2, – , –	–

*Note: DE, RMSE, and MADE have units in mmHg; – means not reported.

A. *Efficacy of the Diastolic Pressure Estimation Model*

Comparing our sitting DBP estimation results with other state-of-the-art, we achieve satisfying results. More importantly, our model meets both the AAMI standard and British Hypertension Society protocol [14]. Judging from the DE, both the mean and STD are less than 5 mmHg; considering MADE, the number 3.62 mmHg is smaller than 5 mmHg. The difference error distribution is displayed in Fig. 5. Furthermore, the proposed DBP monitoring method outperforms [8] in DE and [7] in RMSE. Concerning the correlation, our model displays high correlation ($r = 0.8$) as visualized in Fig. 6. Our correlation is the same as [7] but not as high as [6]. Nevertheless, our subject number is 19, which is at least twice more than the 8 subjects in [6]. This indicates that our model could be more reliable than Chang et al.'s [6].

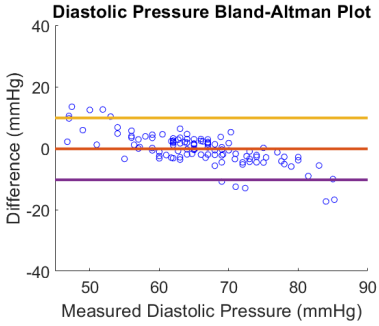

Fig. 5. Bland-Altman plot of the estimated DBP errors.

Six features are selected from the fusion sensors in the final DBP estimation model. They are height, time interval of H-L waves in left carotid horizontal acceleration, time interval of H-J waves in right hand dorsal-ventral acceleration, time interval of J-K waves in right hand dorsal-ventral acceleration, time interval of L-M waves in sternum horizontal acceleration, and magnitude ratio of M-N waves in sternum horizontal acceleration. The linear combinations

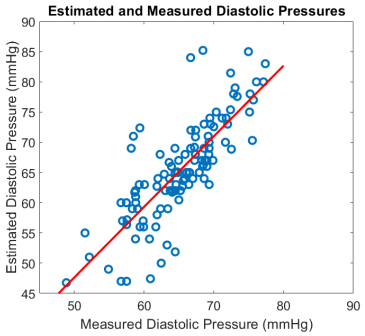

Fig. 6. Demonstration of measured versus estimated DBP.

of the six aforementioned features compose the best DBP estimation model in this study.

B. *Efficacy of the Systolic Pressure Estimation Model*

Judging the performance of the sitting SBP estimation models, we accomplish meeting both the AAMI standard and British Hypertension Society protocol [14]. For the DE, both the mean and STD are less than 8 mmHg; considering MADE, 4.73 mmHg is smaller than 5 mmHg. The difference error distribution is displayed in Fig. 7. Furthermore, the proposed SBP monitoring method beats [6], [8], [9] in DE and [7], [6] in RMSE. Concerning the correlation, our model displays high correlation ($r = 0.81$) as demonstrated in Fig. 8. Our correlation is slightly higher than [7] but not as high as [6], which might be caused by different human subject numbers.

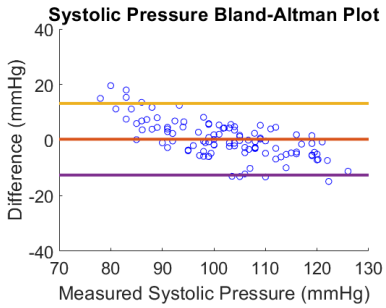

Fig. 7. Bland-Altman plot of the estimated SBP errors.

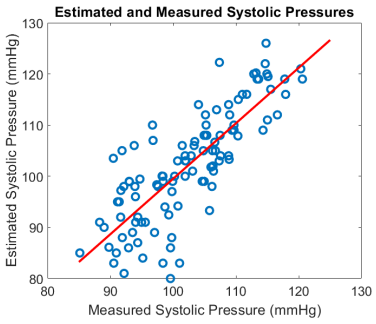

Fig. 8. Demonstration of measured versus estimated SBP.

Five features are chosen from the fusion sensors in the final SBP estimation model. They are height, time interval of K-L waves in sternum horizontal acceleration, time interval of H-L waves in heart horizontal acceleration, time interval of H-J waves in left carotid horizontal acceleration, and time interval of K-M waves in left carotid dorsal-ventral acceleration. The linear combinations of these five features build the best SBP estimation model.

C. Potential of Motion Artifact Resilient Blood Pressure Monitoring

We demonstrate the promising results of motion artifact resilient BP estimation models in Table II, Fig. 9 and Fig. 10. Based on the comparable DE, RMSE, and MADE in standing and walking activities, we could reasonably deduce that robust features have been employed to establish the BP monitoring systems. From the figures, we can clearly observe the logical trends of the BP. Participants with high BP in sitting also have high BP in standing and walking, and vice versa. Future work is encouraged to discover the association between the underlying physiology and the selected robust features.

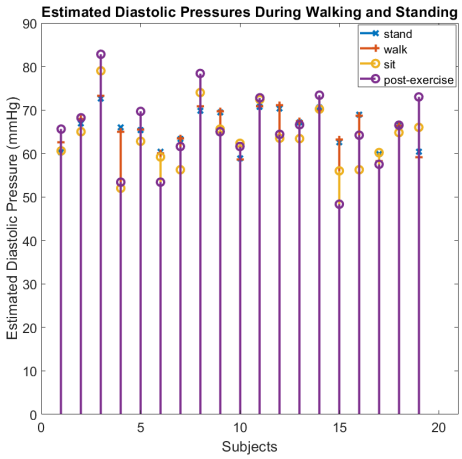

Fig. 9. Demonstration of estimated DBP during motions.

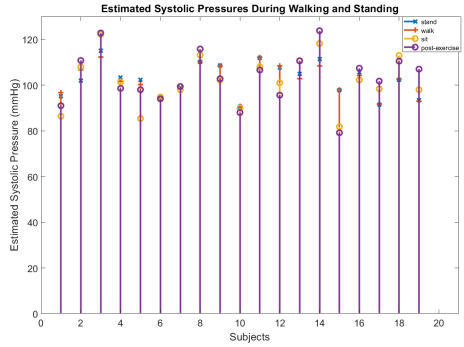

Fig. 10. Demonstration of estimated SBP during motions.

IV. CONCLUSIONS

We present a motion artifact resilient monitoring system for both systolic and diastolic blood pressures. The model fulfills both the AAMI standard and British Hypertension Society protocol. Moreover, we demonstrate that the devised approach is low-cost and convenient. Based on the promising results, we suggest applying the proposed technique in medical usage such as hypertension monitoring and blood pressure variation quantification for targeted diseases.

REFERENCES

[1] A. J. Adler, D. Prabhakaran, P. Bovet, D. S. Kazi, G. Mancia, V. Mungal-Singh, and N. Poulter, "Reducing cardiovascular mortality through prevention and management of raised blood pressure," *A World Heart Federation Roadmap. Global Heart*, vol. 10, no. 2, pp. 111–122, 2015.

[2] D. Perloff, C. Grim, J. Flack, E. D. Frohlich, M. Hill, M. McDonald, and B. Z. Morgenstern, "Human blood pressure determination by sphygmomanometry." *Circulation*, vol. 88, no. 5, pp. 2460–2470, 1993.

[3] B. P. Imholz, W. Wieling, G. A. van Montfrans, and K. H. Wesseling, "Fifteen years experience with finger arterial pressure monitoring: assessment of the technology," *Cardiovascular research*, vol. 38, no. 3, pp. 605–616, 1998.

[4] B. S. Alpert, D. Quinn, and D. Gallick, "Oscillometric blood pressure: a review for clinicians," *Journal of the American Society of Hypertension*, vol. 8, no. 12, pp. 930–938, 2014.

[5] G. Drzewiecki, J. Melbin, and A. Noordergraaf, "Deformational forces in arterial tonometry," in *IEEE TRANSACTIONS ON BIOMEDICAL ENGINEERING*, vol. 31, no. 8. IEEE-INST ELECTRICAL ELECTRONICS ENGINEERS INC 345 E 47TH ST, NEW YORK, NY, 1984, pp. 576–576.

[6] E. Chang, C.-K. Cheng, A. Gupta, P.-H. Hsu, P.-Y. Hsu, H.-L. Liu, A. Moffitt, A. Ren, I. Tsaur, and S. Wang, "Cuff-less blood pressure monitoring with a 3-axis accelerometer," in *2019 41st Annual International Conference of the IEEE Engineering in Medicine and Biology Society (EMBC)*. IEEE, 2019, pp. 6834–6837.

[7] C.-S. Kim, A. M. Carek, O. Inan, R. Mukkamala, and J.-O. Hahn, "Ballistocardiogram-based approach to cuff-less blood pressure monitoring: Proof-of-concept and potential challenges," *IEEE Transactions on Biomedical Engineering*, 2018.

[8] C. Poon and Y. Zhang, "Cuff-less and noninvasive measurements of arterial blood pressure by pulse transit time," in *Engineering in Medicine and Biology Society, 2005. IEEE-EMBS 2005. 27th Annual International Conference of the*. IEEE, 2006, pp. 5877–5880.

[9] Y.-L. Zheng, B. P. Yan, Y.-T. Zhang, and C. C. Poon, "An armband wearable device for overnight and cuff-less blood pressure measurement," *IEEE transactions on biomedical engineering*, vol. 61, no. 7, pp. 2179–2186, 2014.

[10] K. Pandia, S. Ravindran, R. Cole, G. Kovacs, and L. Giovangrandi, "Motion artifact cancellation to obtain heart sounds from a single chest-worn accelerometer," in *2010 IEEE International Conference on Acoustics, Speech and Signal Processing*. IEEE, 2010, pp. 590–593.

[11] P.-Y. Hsu and C.-K. Cheng, "R-peak detection using a hybrid of gaussian and threshold sensitivity," in *2020 42nd Annual International Conference of the IEEE Engineering in Medicine & Biology Society (EMBC)*. IEEE, 2020, pp. 4470–4474.

[12] O. T. Inan, M. Etemadi, R. M. Wiard, L. Giovangrandi, and G. Kovacs, "Robust ballistocardiogram acquisition for home monitoring," *Physiological measurement*, vol. 30, no. 2, p. 169, 2009.

[13] O. T. Inan, P.-F. Migeotte, K.-S. Park, M. Etemadi, K. Tavakolian, R. Casanella, J. Zanetti, J. Tank, I. Funtova, G. K. Prisk, *et al.*, "Ballistocardiography and seismocardiography: A review of recent advances," *IEEE journal of biomedical and health informatics*, vol. 19, no. 4, pp. 1414–1427, 2014.

[14] E. O'brien, B. Waeber, G. Parati, J. Staessen, and M. G. Myers, "Blood pressure measuring devices: recommendations of the european society of hypertension," *BMJ: British Medical Journal*, vol. 322, no. 7285, p. 531, 2001.